Antagonism of CXCR3 Inhibits Lung Metastasis in a Murine Model of Metastatic Breast Cancer

Tonya C. Walser,[1] Salah Rifat,[1] Xinrong Ma,[1] Namita Kundu,[1] Chris Ward,[2] Olga Goloubeva,[3] Michael G. Johnson,[4] Julio C. Medina,[4] Tassie L. Collins,[4] and Amy M. Fulton[1,3]

[1]Department of Pathology, University of Maryland School of Medicine, [2]University of Maryland School of Nursing, and [3]University of Maryland Greenebaum Cancer Center, Baltimore, Maryland; and [4]Amgen, South San Francisco, California

Abstract

Tumor cells aberrantly express chemokines and/or chemokine receptors, and some may promote tumor growth and metastasis. We examined the expression and function of chemokine receptor CXCR3 in a syngeneic murine model of metastatic breast cancer. By flow cytometry, CXCR3 was detected in all murine mammary tumor cell lines examined. All human breast cancer cell lines examined also expressed CXCR3, as did the immortalized but nontumorigenic MCF-10A cell line. Interaction of CXCR3 ligands, CXCL9, CXCL10, and CXCL11, with CXCR3 on the highly malignant murine mammary tumor cell line 66.1 resulted in intracellular calcium mobilization and chemotaxis *in vitro*. To test the hypothesis that tumor metastasis is facilitated by CXCR3 expressed by tumor cells, we employed a small molecular weight antagonist of CXCR3, AMG487. 66.1 tumor cells were pretreated with AMG487 prior to i.v. injection into immune-competent female mice. Antagonism of CXCR3 on 66.1 tumor cells inhibited experimental lung metastasis, and this anti-metastatic activity was compromised in mice depleted of natural killer cells. Systemic administration of AMG487 also inhibited experimental lung metastasis. In contrast to the antimetastatic effect of AMG487, local growth of 66.1 mammary tumors was not affected by receptor antagonism. These studies indicate that murine mammary tumor cells express CXCR3 which facilitates the development of lung metastases. These studies also indicate for the first time that a small molecular weight antagonist of CXCR3 has the potential to inhibit tumor metastasis. (Cancer Res 2006; 66(15): 7701-7)

Introduction

Control of metastasis is the greatest clinical challenge in the treatment of breast cancer. Tumor cells aberrantly express chemokines and/or chemokine receptors, and the interaction of chemokine ligand-receptor pairs is increasingly implicated as a mediator of tumor growth and metastasis. Most notably, a CXCR4-CXCL12 gradient may drive CXCR4-expressing tumor cells to specific metastatic sites where CXCL12, the CXCR4 ligand, is abundantly expressed (1, 2). CXCR4 expressed by tumor cells may also interact with CXCL12 to facilitate tumor growth and escape from oxygen starvation–induced apoptosis (3–7). In several malignancies, tumor cell expression of chemokine receptors is associated with more aggressive disease and poorer prognosis (8–11). Similar to CXCR4, CXCR3 has now been identified in a variety of malignant cells, including melanoma, breast and prostate carcinomas, neuroblastoma, and a subset of B cell lymphomas (12–17). The functional significance and clinical implications of CXCR3 expression by tumor cells remain to be determined.

CXCR3 is expressed by breast adenocarcinoma cell lines (12). Receptor expression is up-regulated by low-serum conditions and, surprisingly, by stimulation with the CXCR3 ligand, CXCL10. Expression of both CXCR3 and CXCL10 by the same tumor cell lines suggests that growth and survival of tumor cells may be regulated by a CXCR3-CXCL10 autocrine loop. Melanoma cells also express CXCR3, and stimulation with the CXCR3 ligand, CXCL9, was shown to activate pathways associated with proliferation and migration, such as integrin VLA-5- and VLA-4-dependent adhesion and RhoA- and Rac1-induced cytoskeletal rearrangements (16). The relevance of CXCR3 to melanoma metastasis was determined by gene silencing with antisense RNA (15). Mice injected with CXCR3-silenced B16 melanoma cells developed fewer lymph node metastases than mice injected with control tumor cells. In contrast to the effects on lymph node metastasis, the extent of lung metastasis was not affected by CXCR3 gene silencing, indicating that CXCR3 mediates organ-specific metastasis in this model. Additionally, mice treated with Freund's adjuvant to increase levels of CXCL9 and CXCL10 in the draining lymph node experienced a slight increase in lymph node metastasis of melanoma cells. Taken together, these initial studies of CXCR3 expression by malignant cells indicate that CXCR3-expressing tumor cells may migrate to specific metastatic sites where CXCR3 ligands, CXCL9, CXCL10, and CXCL11, are expressed. Similar to CXCR4, CXCR3 expressed by tumor cells may also interact with CXCR3 ligands within local tumors to promote tumor cell growth and survival.

In the current study, we used a murine model of metastatic breast cancer to examine CXCR3 expression and function. Using a small molecular weight pharmacologic CXCR3 antagonist, we determined the effect of tumor-specific CXCR3 blockade and systemic CXCR3 blockade on tumor behavior. We also examined the role of host immunity in the therapeutic effects mediated by CXCR3 antagonism.

Materials and Methods

Murine tumor cell lines. Tumor cell lines 66.1 and 410 were derived from a spontaneously occurring mammary adenocarcinoma in a BALB/cfC3H mouse (18). Tumor cell line 410.4 was derived from a pulmonary lesion of a mouse implanted with 410 tumor cells. 66.1 and 410.4 are highly tumorigenic and metastatic following both s.c. and i.v. injection into mice. 410 is tumorigenic but rarely metastatic. Murine tumor cell lines are grown in DMEM, supplemented with 10% fetal bovine serum (FBS; Gemini Bioproducts, Woodland, CA), 1.5 mg/mL sodium bicarbonate, 2 mmol/L

Requests for reprints: Amy M. Fulton, Department of Pathology, University of Maryland School of Medicine, 10 South Pine Street, Baltimore, MD 21201. Phone: 410-706-6479; Fax: 410-706-8414; E-mail: afulton@umaryland.edu.

doi:10.1158/0008-5472.CAN-06-0709

L-glutamine, 100 μmol/L nonessential amino acids, 100 units/mL penicillin, and 100 units/mL streptomycin in a 10% CO_2 atmosphere.

Human cell lines. MCF-10A is an immortalized nontumorigenic epithelial cell line derived from tissue from a reduction mammoplasty. MCF-7, MDA-MB-231, and MDA-MB-468 are tumor cell lines derived from the pleural effusions of patients with breast adenocarcinomas, whereas T-47D is a tumor cell line derived from the pleural effusion of a patient with ductal breast carcinoma. All of the human cell lines, except MCF-10A, are grown in the growth medium described for murine tumor cell lines but in a 5% CO_2 atmosphere. MCF-10A is grown in equal parts DMEM (with 4.5 g/L glucose and without L-glutamine) and HyQ Ham's F-12, supplemented with 5% horse serum (Biosource, Camarillo, CA), 10 μg/mL insulin, 500 ng/mL hydrocortisone, 100 ng/mL cholera toxin, and 20 ng/mL epidermal growth factor in a 5% CO_2 atmosphere.

Syngeneic models of tumorigenicity and lung metastasis. Local tumor growth and spontaneous metastasis were evaluated by injecting 3×10^5 viable tumor cells s.c. proximal to the right abdominal mammary gland of syngeneic female mice. Tumor diameters were measured by caliper twice weekly, and mice were euthanized on an individual basis when the s.c. tumor measured 18 mm in diameter or earlier if the mouse seemed moribund. The lungs were removed and weighed, and surface tumor colonies were quantified in a blinded fashion under a dissecting microscope. Experimental metastasis was evaluated by injecting 9×10^4 viable tumor cells i.v. into the lateral tail vein of syngeneic female mice. All mice were euthanized on day 21 posttransplantation or earlier if the mice seemed moribund. The lungs were removed and weighed, and surface tumor colonies were quantified in a blinded fashion under a dissecting microscope.

Mice. BALB/cByJ female mice were purchased from the Jackson Laboratory, Bar Harbor, ME. C.B-17/IcrCrl-SCID/Br [severe combined immunodeficiency (SCID); on a BALB/c background] female mice were purchased from Charles River Laboratories, Wilmington, MA. For studies requiring natural killer (NK) cell depletion, mice were given an i.p. injection of rabbit asialo-GM1 ganglioside antibody (Wako Bioproducts, Richmond, VA) in 500 μL of saline. Anti-NK cell treatments were administered on days −1 and +3 relative to tumor cell injection. In the current study, this protocol depletes 50% to 70% of the NK cells normally found in the spleen. All mice were housed, cared for, and used in strict accordance with USDA regulations and the NIH Health Guide for the Care and Use of Laboratory Animals. The University of Maryland School of Medicine Animal Facility is fully accredited by the American Association for the Accreditation of Laboratory Animal Care.

Flow cytometry. For surface receptor staining, cells were fixed in 1% paraformaldehyde for 30 minutes at 4°C, and then blocked with 5% FBS for 30 minutes at 4°C. For intracellular receptor staining, the initial fixation was in 70% ethanol instead of 1% paraformaldehyde. Cells were stained with PE-labeled rat anti-mouse CXCR3 monoclonal antibody (220803), PE-labeled mouse anti-human CXCR3 monoclonal antibody (49801), or manufacturer-recommended isotype control antibody (IC006P and IC002P, respectively; all R&D Systems, Minneapolis, MN) for 45 minutes at 4°C. Histograms representing specific staining and isotype control staining were overlaid, and a marker was placed at the integration point of the two histograms.

Reverse transcription PCR. Total RNA was extracted using TRIzol Reagent (Invitrogen, Carlsbad, CA) according to the manufacturer's instructions. Total RNA (3 μg) was reverse-transcribed to cDNA using SuperScript II RNase H Reverse Transcriptase, and 2 μL of the cDNA product was amplified by PCR using Platinum Blue PCR SuperMix (both Invitrogen). The sequences of the gene-specific primers were as follows: CXCR3 forward 5′-aaaacagcacctctcccta-3′, CXCR3 reverse 5′-tctgaacttcactccccaca-3′; β-actin forward 5′-gtgggccgctctaggcaccaa-3′, β-actin reverse 5′-tacgaccagaggcatacag-3′. The PCR protocol included an initial denaturation at 94°C for 3 minutes, followed by 30 cycles of PCR as follows: denaturation at 94°C for 30 seconds, annealing at 56°C for 45 seconds, and extension at 72°C for 30 seconds. The reaction was completed at 72°C for 8 minutes. The PCR amplification products were analyzed on a 1% agarose gel stained with ethidium bromide and were visualized by EV epifluorescence.

Calcium flux imaging. Tumor cells were seeded in glass-bottomed 35-mm dishes (MatTek, Ashland, MA) coated with a solution of 2.5 μg/mL of fibronectin. Tumor cells growing in culture were loaded with 5 μmol/L of fluo-3 AM in phenol red–free DMEM supplemented with 25 mmol/L HEPES (base medium) for 30 minutes and then rinsed in base medium alone for 30 minutes to allow complete de-esterification of the AM dye. Agonist-initiated calcium flux was assayed using an Olympus IX-70 microscope (×60-1.2 NA water objective; Olympus, Melville, NY) coupled to a Bio-Rad Radiance 2100 laser scanning confocal system (488 nm excitation; Bio-Rad Laboratories, Hercules, CA) operated in xy mode (1 Hz). Tumor cells were imaged in base medium alone followed by bath application of 10 μg/mL recombinant murine (rm) CXCL9, rmCXCL10, or rmCXCL11 (all PeproTech, Rock Hill, NJ). Approximately 120 seconds after agonist challenge, 2 μmol/L of ionomycin was added to serve as an internal positive control. In a separate set of experiments, the addition of base medium alone served as the negative or buffer change control. Cell fluorescence was analyzed by manually identifying regions of interest in 12 to 25 cells within each field using a customized program written in IDL (Kodak, Rochester, NY). Temporal fluorescence responses were background-corrected and calculated as mean fluorescence within each region of interest at each time point (1 Hz).

Chemotaxis assay. Nucleopore polycarbonate membranes (Whatman, Clifton, NJ) with an 8 μm pore size were coated with a solution of 500 ng/mL fibronectin and 25 μg/mL collagen I and assembled into 24-well plates of modified Boyden chambers. Detached tumor cells were loaded with 50 μg/mL of calcein AM (Molecular Probes, Eugene, OR) in phenol red–free DMEM supplemented with 25 mmol/L of HEPES (base medium) for 1 hour at 37°C. Dye-loaded tumor cells (1×10^5) were added to the upper compartments of the modified Boyden chambers, and various concentrations of rmCXCL9, rmCXCL10, or rmCXCL11 (all from PeproTech) were added to the lower compartments. The positive control chemoattractant was 2% FBS, and the negative control chemoattractant was base medium alone. Dye-loaded tumor cells (1×10^5) were added to the lower compartments of several wells for use as assay standards. After incubation for 6 hours at 37°C, nonmigrating cells were poured from the upper compartment, residual cells were removed using a cotton-tipped swab, and the upper compartment was returned to the appropriate well. The entire plate was measured for fluorescence at 485 nm, and the results are expressed as mean number of cells migrated.

AMG487 formulation. AMG487 was kindly provided by Amgen, South San Francisco, CA. The *in vitro* formulation of AMG487 was prepared as a 10 mmol/L stock with DMSO. Tumor cells growing in culture were washed, and fresh growth medium containing 200 nmol/L AMG487, 1 μmol/L AMG487, or DMSO vehicle was returned to the dish for 18 hours at 37°C. The tumor cells were washed and processed as usual for injection into mice. The *in vivo* formulation of AMG487 was used to s.c. treat mice twice daily at 5 mg/kg. Briefly, a 50% hydroxypropyl-β-cyclodextrin (Sigma, St. Louis, MO) solution was prepared; at 20%, this solution served as the vehicle. AMG487 was added to the 50% solution, and it was incubated in a sonicating water bath for 2 hours with occasional vortexing. Distilled water was added to give the appropriate final concentration of AMG487 in 20% of hydroxypropyl-β-cyclodextrin.

Statistical analysis. The general linear model approach was used for the analyses of lung metastases and lung weight data. All experiments were analyzed separately. To assure approximate normality, a square root transformation was used for the lung metastases data. Dunnett's procedure was used for pairwise group comparisons. Differences statistically significant at the 0.05 level were reported as estimated difference in groups' means with the corresponding 95% confidence interval. Descriptive statistics are reported as mean ± SE.

Results

Characterization of CXCR3 expression by tumor epithelial cell lines. We surveyed four human breast cancer cell lines (MCF-7, T-47D, MDA-MB-231, and MDA-MB-468) and one nontransformed human breast epithelial cell line (MCF-10A) for expression of

CXCR3. By flow cytometry, all of the human cell lines stained positive for surface CXCR3 (11-68%; Fig. 1*A*). Although the percentage of positive cells varied from experiment to experiment, nontransformed breast epithelial cell line MCF-10A consistently expressed the lowest level of CXCR3 (11%) compared with the breast cancer cell lines. Likewise, we surveyed metastatic (66.1 and 410.4) and nonmetastatic (410) murine mammary tumor cell lines for CXCR3 expression. Each of the murine mammary tumor cell lines expressed surface CXCR3 (22-31%; Fig. 1*B*). Interestingly, when cells were permeabilized before they were stained, many more were positive for CXCR3; 50% to 78% of cells of the human breast cell lines and 87% to 93% of cells of the murine mammary tumor cell lines stained positive for intracellular CXCR3 (data not shown). CXCR3 mRNA expression was confirmed by reverse transcription PCR. RNA extracted from cultured murine mammary tumor cells was probed with primers specific for CXCR3 or β-actin. Consistent with the protein data, CXCR3 mRNA was detected in each of the murine mammary tumor cell lines (Fig. 1*C*).

Functional studies of CXCR3 on 66.1 tumor cells. To determine if CXCR3 was functional on murine mammary tumor cells, we asked if ligand stimulation would mobilize intracellular calcium. Figure 2*A* shows select still images from video taken of calcium mobilization in 66.1 tumor cells in response to stimulation with 10 μg/mL of rmCXCL11. 66.1 tumor cells fluoresce after exposure to 10 μg/mL of CXCL11. Ionomycin was included as a positive control. Likewise, 66.1 tumor cells fluoresce after exposure to 10 μg/mL of CXCL9 or 10 μg/mL of CXCL10 (data not shown). Figure 2*B* shows the quantification of calcium mobilization in 66.1 tumor cells in response to 10 μg/mL of CXCL9, CXCL10, or CXCL11. A negative or buffer change control is also shown for comparison. All of the ligands induced calcium mobilization in 66.1 tumor cells but to varying degrees. CXCL10 and CXCL11 generated similarly robust responses, whereas CXCL9 was less effective at stimulating calcium flux.

Directed migration of cells bearing chemokine receptors to sites of ligand expression is another indicator of receptor function. 66.1 tumor cells were harvested, loaded with a fluorescent indicator, placed in modified Boyden chambers, and allowed to migrate toward various concentrations of CXCL9, CXCL10, CXCL11, or base medium alone. 66.1 tumor cells migrated to each of the chemokines preferentially and in a dose-dependent manner compared with base medium alone (Fig. 3*A-C*). The peak response to CXCL9, CXCL10, and CXCL11 occurred at 10 to 100 ng/mL. These calcium mobilization and chemotaxis assays indicate that CXCR3 expressed on the surface of 66.1 tumor cells is functionally coupled to intracellular signaling events.

The effects of tumor cell CXCR3 antagonism. To test the hypothesis that antagonism of CXCR3 expressed on tumor cells would inhibit metastasis of the tumor cells to lungs, a specific small molecular weight antagonist of CXCR3, AMG487, was employed. AMG487 blocks *in vitro* lymphocyte migration mediated by CXCL9, CXCL10, or CXCL11,[5] however, it has not been evaluated in a cancer model. To avoid confounding effects of the antagonist on host CXCR3, 66.1 tumor cells were pretreated with 200 nmol/L of AMG487, 1 μmol/L of AMG487, or vehicle for 18 hours *in vitro*. The tumor cells were then washed and injected i.v. into syngeneic BALB/cByJ mice. Twenty-one days later, mice were euthanized, and lungs were examined for metastases. Tumor cells treated with

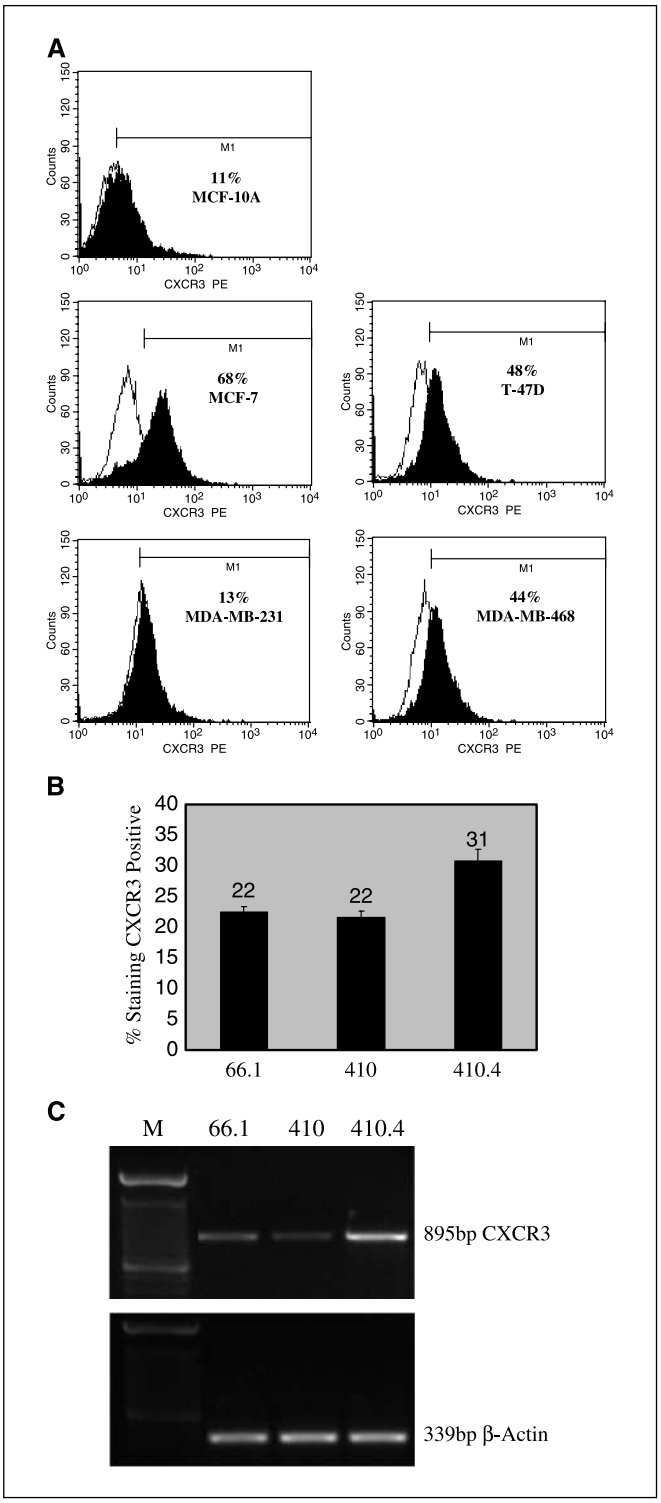

Figure 1. *A-C,* flow cytometry and PCR detection of CXCR3. *A,* four human breast cancer cell lines and one nontransformed breast epithelial cell line (*MCF-10A*) were stained for surface CXCR3 and analyzed by flow cytometry. *Solid histogram,* CXCR3 staining; *clear histogram,* isotype staining. Data reported as the percentage of total cells staining positive for CXCR3 when a marker is placed at the integration point of overlaid histograms. *B,* two metastatic (66.1 and 410.4) and one nonmetastatic (410) murine mammary tumor cell lines were stained for surface CXCR3 and analyzed by flow cytometry. *Columns,* percentage of total cells staining positive for CXCR3 (two replicates each); *bars,* ±SE. *C,* RNA isolated from two metastatic (66.1 and 410.4) and one nonmetastatic (410) murine mammary tumor cell lines was reverse-transcribed, and the resulting cDNA was amplified by PCR using primers specific for CXCR3 or β-actin.

[5] T.L. Collins, M.G. Johnson, and J.C. Medina, unpublished data.

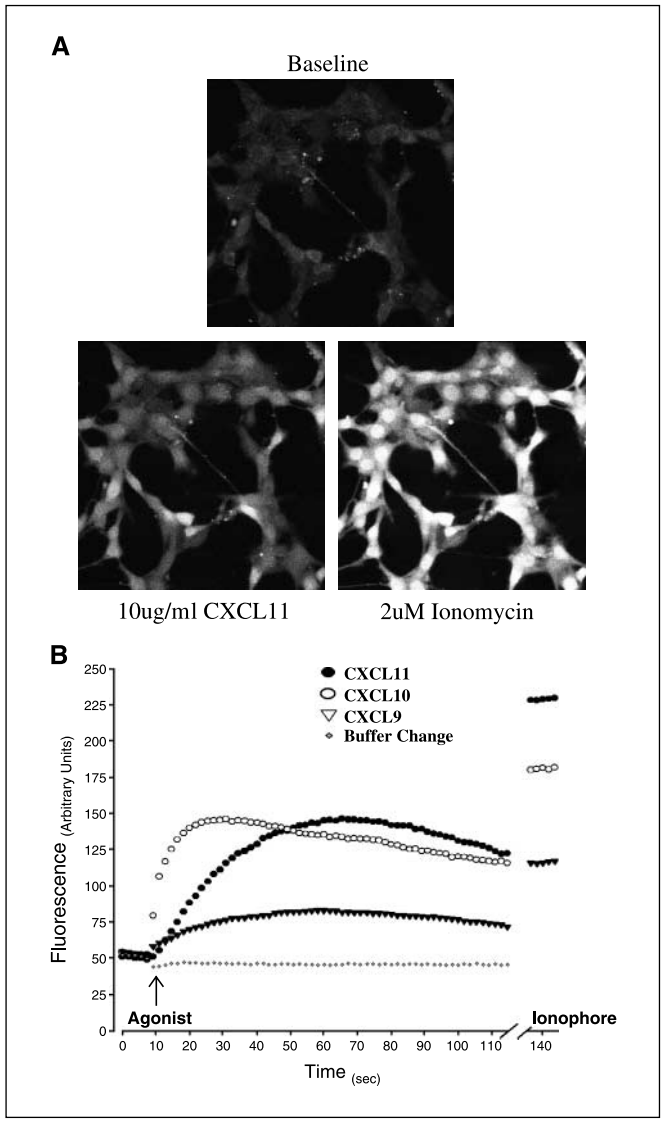

Figure 2. *A-B,* CXCL9-, CXCL10-, or CXCL11-stimulated calcium mobilization in 66.1 tumor cells. 66.1 tumor cells were loaded with the fluorescent indicator fluo-3 AM and stimulated with 10 μg/mL CXCL9, CXCL10, or CXCL11, and fluorescent images were collected. Ionomycin served as the positive control agonist. The addition of base medium alone served as the negative or buffer change control. Calcium mobilization is defined as increased fluorescent intensity of cells. *A,* the baseline image was captured prior to the addition of agonist. The 10 μg/mL rmCXCL11 image was captured 20 seconds after the addition of CXCL11. The 2 μmol/L ionomycin image was captured immediately after the addition of the ionophore ionomycin. *B,* regions of interest in 12 to 25 cells within each field were manually identified and analyzed using a customized program written in IDL. Temporal fluorescence responses were background-corrected and calculated. *Points,* mean fluorescence within each region of interest at each time point.

1 μmol/L of AMG487 developed into fewer lung metastases than vehicle-treated tumor cells (40 versus 104 metastases; $P < 0.001$; Fig. 4*A*). The lower dose of AMG487 was not therapeutic. The weights of the lungs showed the same trend; 1 μmol/L AMG487 lungs were significantly smaller than vehicle lungs, where the estimated difference in the group means is 0.05 g with the corresponding 95% confidence interval (0.002-0.096 g; data not shown).

To rule out the possibility that AMG487 inhibits lung metastases because it is cytotoxic to tumor cells, a proliferation assay was done where 66.1 tumor cells growing in culture were treated with 200 nmol/L of AMG487, 1 μmol/L of AMG487, 10 μmol/L of AMG487, or vehicle or were left untreated. The CXCR3 antagonist did not affect proliferation of the tumor cells at 24, 48, or 72 hours under normal or serum-free growth conditions (data not shown). AMG487 did, however, inhibit the migration of 66.1 tumor cells to CXCL9 by ~70% (data not shown).

The effects of systemic CXCR3 antagonism. Systemic drug treatment also inhibited experimental lung metastases. 66.1 tumor cells were injected i.v., and mice were treated twice daily on days −1 to +7 with s.c. injections of 5 mg/kg of AMG487 or vehicle. When the lungs were examined on day 21 posttransplantation, AMG487-treated mice had developed fewer metastases than vehicle-treated mice (113 versus 171 metastases; $P = 0.01$; Fig. 4*B*).

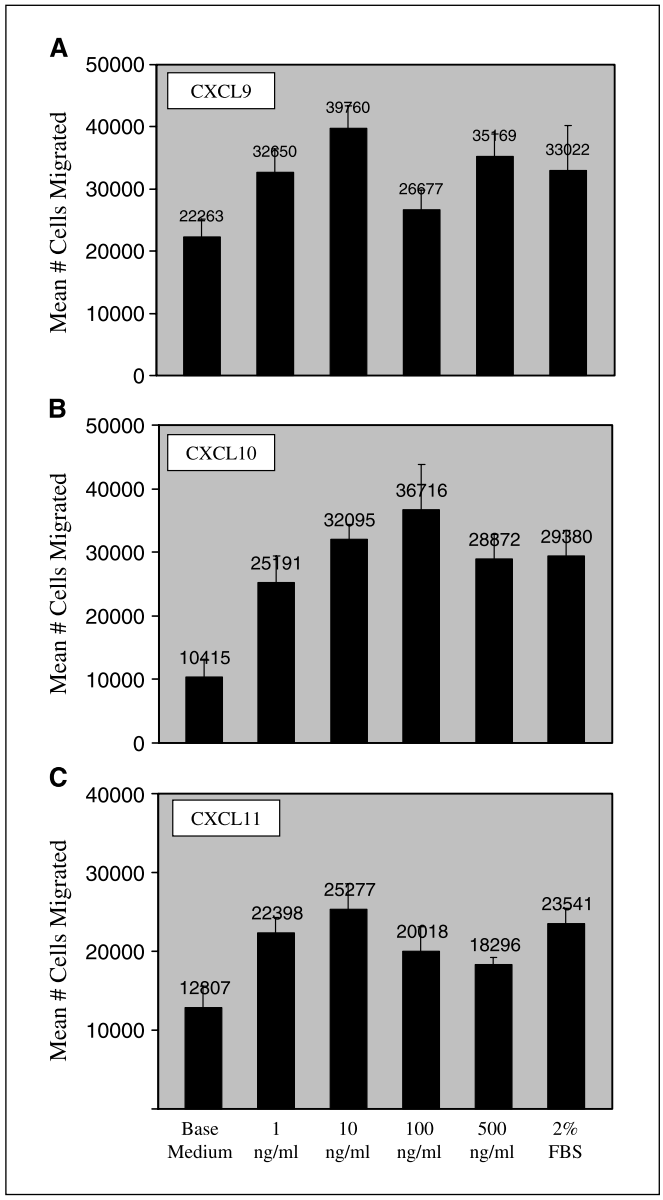

Figure 3. *A-C,* migration of 66.1 tumor cells to various concentrations of CXCL9, CXCL10, or CXCL11. 66.1 tumor cells were loaded with the fluorescent indicator calcein AM, placed in modified Boyden chambers, and allowed to migrate toward 1, 10, 100, or 500 ng/mL of (*A*) CXCL9, (*B*) CXCL10, or (*C*) CXCL11. FBS (2%) served as the positive control chemoattractant, and base medium alone served as the negative control chemoattractant. *Columns,* mean number of cells migrated (six replicates each); *bars,* ±SE.

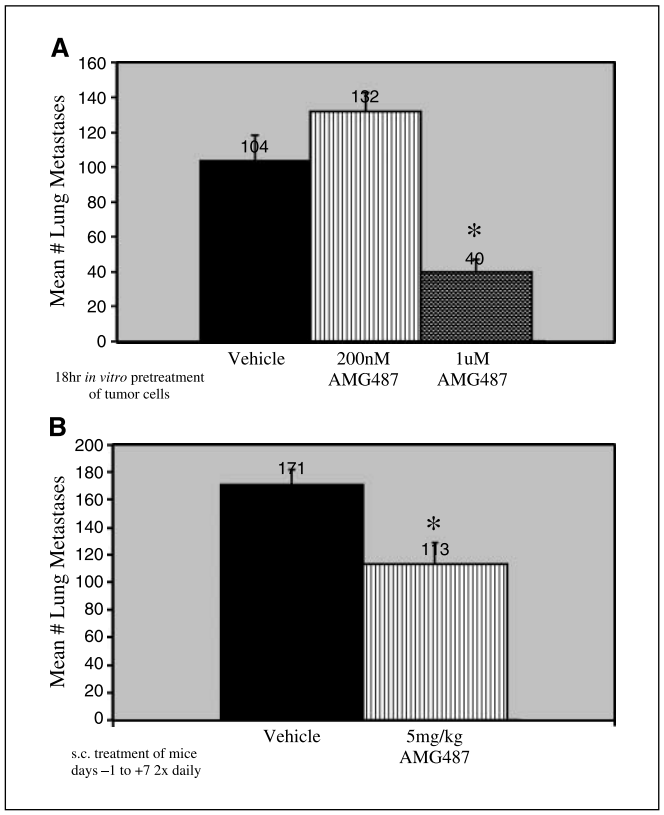

Figure 4. *A-B,* experimental lung metastases after tumor-specific or systemic blockade of CXCR3 with the antagonist AMG487. *A,* 66.1 tumors cells growing in culture were treated 18 hours with 200 nmol/L AMG487, 1 μmol/L AMG487, or vehicle. The treatment was washed away, and 9×10^4 66.1 tumor cells of each treatment type were injected i.v. into BALB/cByJ female mice. *B,* 9×10^4 untreated 66.1 tumor cells were injected i.v. into BALB/cByJ female mice. The mice were treated s.c. with 5 mg/kg AMG487 or vehicle twice daily on days −1 to +7 posttransplantation. All mice were euthanized on day 21 posttransplantation or earlier if the mice seemed moribund. *Columns,* mean number lung metastases (10 mice per group); *bars,* ±SE. $P < 0.001$, AMG487 versus vehicle (1 μmol/L). $P < 0.01$, AMG487 versus vehicle (5 mg/kg).

Although 66.1 tumors grow progressively in immune-competent mice, it is possible that some endogenous growth control is mediated by host immune effector cells, including CXCR3-positive T cells and NK cells. We were concerned that systemic CXCR3 antagonism with AMG487 might subvert this endogenous control and cause local tumors to behave more aggressively. To test this, 66.1 tumor cells were injected s.c. proximal to the right abdominal mammary gland of mice, AMG487 was administered to mice systemically, and local tumor growth was monitored. Mice were treated twice daily on days 0 to 28 with s.c. injections of 5 mg/kg AMG487 or vehicle. Systemic treatment of mice with 5 mg/kg AMG487 did not adversely affect local tumor growth (Fig. 5*A*). Tumor size was comparable in AMG487- and vehicle-treated mice. When the lungs were examined for spontaneous metastases, AMG487-treated mice had developed fewer metastases than vehicle-treated mice (85 versus 112 metastases; Fig. 5*B*). The difference in the mean number of lung metastases was not statistically significant ($P = 0.29$), however, a trend towards protection from metastatic disease was observed, consistent with the antimetastatic effect observed in Fig. 4*A* and *B*.

Immune-dependent AMG487-mediated inhibition of experimental lung metastasis. To determine if host cells play a role in the antimetastatic activity of AMG487, therapy was compared in immune-competent mice, mice depleted of NK cells, and mice lacking functional T cells (SCID mice). Mice were injected i.v. with 66.1 tumor cells pretreated with 1 μmol/L AMG487 or vehicle for 18 hours *in vitro.* Immune-competent mice injected with AMG487-treated tumor cells developed fewer lung metastases than mice injected with vehicle-treated tumor cells, confirming the antimetastatic activity of AMG487 (98 versus 190 metastases; $P = 0.02$; Fig. 6). When the host was depleted of NK cells, however, all therapy normally conferred by AMG487 was abolished (705 versus 98 metastases; $P < 0.001$). Interestingly, fewer lung metastases were observed in vehicle-treated SCID mice versus vehicle-treated BALB/cByJ mice (156 versus 190 lung metastases), indicating that some T cell population may actually promote metastasis. This confounding effect of T cell depletion made it impossible to determine if AMG487 therapy required T cells.

Discussion

In the proceeding studies, we detected CXCR3 protein expression on human breast cancer cell lines, confirming the report of Goldberg-Bittman et al. (12). Four human breast cancer cell lines consistently expressed more surface receptor than a nontransformed breast epithelial cell line, MCF-10A. We also surveyed a

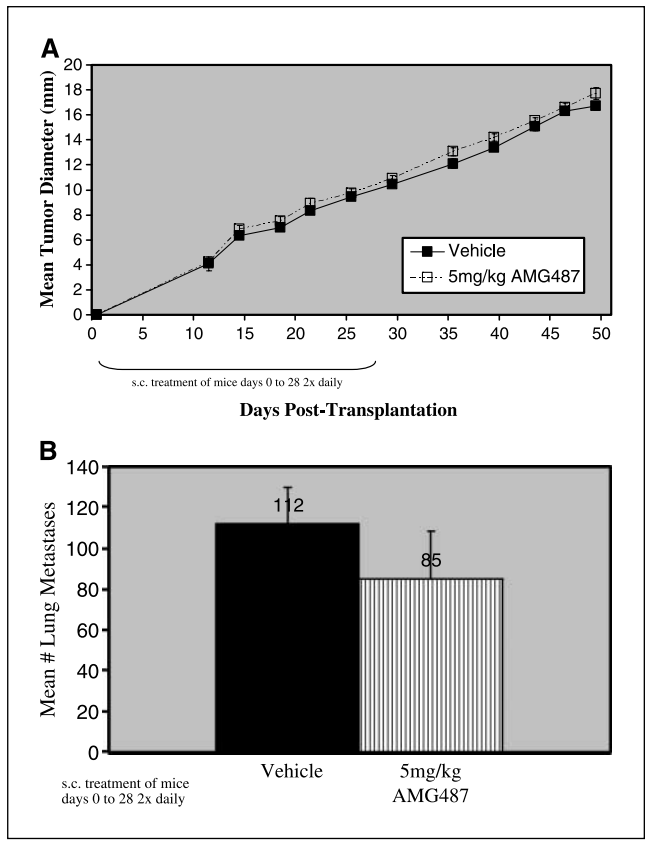

Figure 5. *A-B,* local tumor growth and spontaneous lung metastasis after systemic treatment with AMG487. 66.1 tumor cells (3×10^5) were injected s.c. into BALB/cByJ female mice. The mice were treated s.c. with 5 mg/kg of AMG487 or vehicle twice daily on days 0 to 28 posttransplantation. Each mouse was euthanized on an individual basis when the s.c. tumor measured 18 mm in diameter or earlier if the mouse seemed moribund (10 mice per group). *A,* tumor diameters were measured by caliper twice weekly. *Points,* mean tumor diameter; *bars,* ±SE. *B,* lung tumor colonies were quantified in a blinded fashion under a dissecting microscope. *Columns,* mean number of lung metastases; *bars,* ±SE.

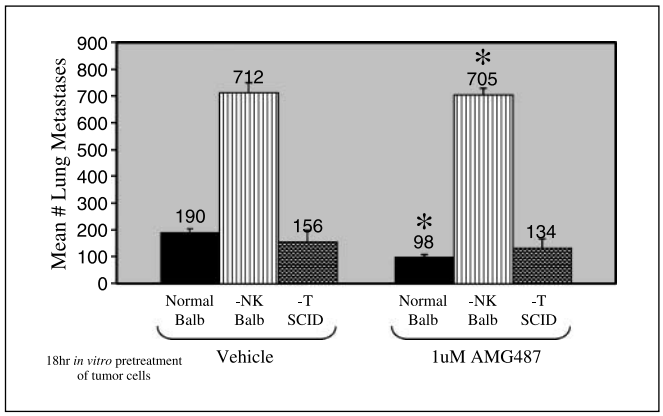

Figure 6. Immune-dependent AMG487-mediated inhibition of experimental lung metastases. 66.1 tumors cells growing in culture were treated 18 hours with 1 μmol/L AMG487 or vehicle. The treatment was washed away, and 9×10^4 66.1 tumor cells of each treatment type were injected i.v. into immune-competent BALB/cByJ mice, BALB/cByJ mice depleted of NK cells, or T cell–deficient BALB/SCID mice. All mice were euthanized on day 21 of posttransplantation or earlier if the mice seemed moribund (10 mice per group). *Columns,* mean number lung metastases; *bars,* ±SE. $P = 0.02$, vehicle/normal BALB versus 1 μmol/L AMG487/normal BALB. $P < 0.001$, 1 μmol/L AMG487/normal BALB versus 1 μmol/L AMG487/-NK BALB.

panel of three murine mammary tumor cell lines of varying metastatic potential for surface CXCR3 expression, and each was positive for the receptor. If cells were fixed prior to staining, surface CXCR3 expression was more readily detected. CXCR3 expression was also detected in much greater abundance in permeabilized cells. These findings suggest that CXCR3 on the surface of tumor cells is transiently expressed and rapidly internalized and sequestered in response to experimental manipulation. Rapid internalization of chemokine receptors is common, and other laboratories have also detected more CXCR3 in permeabilized tumor cells (15, 17). If CXCR3 is important to tumor progression and metastasis, more aggressive tumor cells may simply be better at recruiting CXCR3 as needed to the cell surface from abundant internal pools. The presence of surface CXCR3 on both metastatic and nonmetastatic tumor cells may indicate that the tumor cells acquire CXCR3 expression early in malignant progression. A lack of correlation between surface CXCR3 expression and metastatic potential was also reported in melanoma (15). These findings indicate that CXCR3 contributes to, but is not the ultimate determinate of, metastatic behavior. We examined a limited series of primary human breast tumors by immunohistochemistry and detected strong CXCR3 expression in malignant epithelium. CXCR3 was weak or absent in normal ductal epithelium from the same sections.

We have now shown that CXCR3 is functional on murine mammary tumor cell line 66.1. Each CXCR3 ligand, CXCL9, CXCL10, and CXCL11, stimulated intracellular calcium mobilization in 66.1 tumor cells. We also examined chemotaxis of 66.1 tumor cells in response to stimulation with CXCL9, CXCL10, or CXCL11. 66.1 tumor cells migrated to each of the chemokines. Furthermore, we observed that the chemokines mediated CXCR3 signaling with the following affinities: CXCL11 ≈ CXCL10 > CXCL9. These findings confirm studies from several laboratories showing that CXCR3 on malignant cells mediates intracellular signaling (13, 15, 16, 19).

We postulated that CXCR3 on 66.1 tumor cells aids in the development of metastases at distant sites where CXCL9, CXCL10, or CXCL11 are expressed at higher levels, such as the lungs. Using a small molecular weight antagonist of CXCR3, AMG487, we tested the hypothesis that tumor metastasis is facilitated by tumor cell CXCR3 expression. Similar to tumor cells, however, some host cells express CXCR3, and CXCR3 on both cell types could be antagonized by AMG487. To delineate the effects of antagonizing tumor-CXCR3 versus host-CXCR3, we pretreated 66.1 tumor cells with AMG487 prior to injecting the tumor cells i.v. into mice. The antimetastatic activity observed in this setting indicates that tumor-CXCR3 is a direct target of AMG487, consistent with a mechanism by which tumor-CXCR3 directly promotes metastasis. This therapy is not attributable to a cytotoxic effect of AMG487 on the tumor cells because 66.1 tumor cells growing *in vitro* proliferated normally when exposed to 200 nmol/L to 10 μmol/L AMG487 or vehicle compared with untreated 66.1 tumor cells. Although several laboratories have reported CXCR3 expression in a variety of malignancies, we are aware of only one other report that targeting CXCR3 is protective against metastatic disease (15). In that study, antisense RNA to tumor-CXCR3 inhibited metastasis of B16 melanoma cells to lymph nodes. Inflammatory reactions that increased ligand expression in lymph nodes also increased melanoma metastasis to that tissue. Interestingly, melanoma pulmonary metastasis was not affected by CXCR3 down-regulation. We do not know if the organ-specific effects of tumor-CXCR3 antagonism on melanoma and breast cancer are a function of the malignant cell or the method of receptor blocking. The current study is the first report that a pharmacologic antagonist of CXCR3 has potential as a cancer therapy.

In spite of the promising antimetastatic properties of AMG487, we were concerned that systemic antagonism of CXCR3 might enhance local tumor growth. A number of host cells express CXCR3, including T cells and NK cells. If these cells exert some endogenous control over local tumor growth, systemic receptor antagonism might accelerate the growth of local tumors. We found, however, that systemic antagonism of CXCR3 with AMG487 does not adversely affect local tumor growth or survival. Furthermore, systemic treatment of mice with AMG487 inhibited lung metastases occurring spontaneously in mice bearing orthotopically growing tumors. Systemic treatment of mice with AMG487 also inhibited experimental lung metastases occurring in mice injected i.v. with tumor cells. More studies are required to determine why local tumors are not affected by systemic CXCR3 antagonism, but the lack of an affect on local tumor growth may be a general phenomenon because s.c. growth of B16 melanoma was also not affected by tumor-CXCR3 antisense (15). Little endogenous growth control may be mediated by the host, or the host cell required to control local tumor growth may not be a $CXCR3^+$ T cell or $CXCR3^+$ NK cell. We observed minimal infiltration of 66.1 tumors with $CD4^+$ or $CD8^+$ T cells, and in these populations, only 8% of $CD4^+$ T cells and 18% of $CD8^+$ T cells were also positive for CXCR3. Finally, the concentration of AMG487 required to inhibit host-CXCR3 may be higher than the concentration necessary to inhibit tumor-CXCR3.

Although we postulated that direct antagonism of tumor-CXCR3 would prevent tumor cell migration and survival at distant sites, we considered the possibility that host cells might play a role in this therapy. Our previous studies have indicated that NK cells exert control over tumor metastasis (20, 21). To examine the potential role of NK cells, we compared AMG487 antimetastatic efficacy in immune-competent and NK-depleted mice. When the host was depleted of NK cells, antimetastatic therapy of AMG487 was lost. Thus, in addition to a direct effect on tumor-CXCR3,

AMG487 may affect the interactions of tumors and NK cells. NK cells may mediate antimetastatic activity by killing tumor cells directly or by contributing cytokines critical to host defense against tumor cell growth and metastasis, like IFN-γ. Future studies will determine the precise contributions of NK cells.

Systemically administered AMG487 theoretically blocks CXCR3 on host NK cells just as it blocks tumor-CXCR3, so the dependence of AMG487-mediated therapy on NK cells presents something of a paradox. One possibility is that the concentration of AMG487 required to inhibit host-CXCR3 may be higher than the concentration necessary to inhibit tumor-CXCR3. Another interesting possibility is that the antimetastatic activity of AMG487 is mediated by CXCR3-null NK cells. NK cells present in the peripheral blood or lungs of mice were recently reported to be negative for CXCR3 (22). Systemic administration of AMG487 would not be expected to have an effect on the function of these CXCR3-null NK cells. Future studies will examine these possibilities.

In summary, we have shown that CXCR3 is present and functional on the highly malignant murine mammary tumor cell line 66.1. We have shown for the first time that the use of a small molecular weight antagonist to block CXCR3 on tumor cells inhibits lung metastases. Systemic blockade of CXCR3 also inhibits experimental metastases and, to a lesser extent, spontaneous metastasis, but it does not affect local tumor growth. We are also reporting for the first time that CXCR3 antagonist-based therapy requires functional NK cells. These studies support the hypothesis that tumor cells aberrantly express CXCR3 to facilitate the development of metastases at distant sites of CXCR3 ligand expression. These studies also suggest that tumor cell CXCR3 may not be important to control local tumor behavior.

CXCR3 expression has been reported on a wide range of human malignancies, including breast cancer, and several laboratories have shown that this receptor can mediate migration and invasion *in vitro*. The current studies and those of Kawada et al. (15) indicate that targeting CXCR3 may specifically inhibit tumor metastasis without adversely affecting local tumor growth. Further studies will elucidate the relevant mechanisms to optimize this therapeutic approach.

Acknowledgments

Received 2/27/2006; revised 5/2/2006; accepted 5/11/2006.

Grant support: Susan G. Komen Breast Cancer Foundation grant DISS0201496 (T.C. Walser) and NIH grant CA78394 (A.M. Fulton).

The costs of publication of this article were defrayed in part by the payment of page charges. This article must therefore be hereby marked *advertisement* in accordance with 18 U.S.C. Section 1734 solely to indicate this fact.

We thank the Flow Cytometry Core Facility at the University of Maryland Greenebaum Cancer Center, and Dr. George Tonn at Amgen for assistance with the *in vivo* formulation of AMG487.

References

1. Muller A, Homey B, Soto H, et al. Involvement of chemokine receptors in breast cancer metastasis. Nature 2001;410:50–6.
2. Scotton CJ, Wilson JL, Milliken D, Stamp G, Balkwill FR. Epithelial cancer cell migration: a role for chemokine receptors? Cancer Res 2001;61:4961–5.
3. Bachelder RE, Wendt MA, Mercurio AM. Vascular endothelial growth factor promotes breast carcinoma invasion in an autocrine manner by regulating the chemokine receptor CXCR4. Cancer Res 2002;62:7203–6.
4. Bertolini F, Dell'Agnola C, Mancuso P, et al. CXCR4 neutralization, a novel therapeutic approach for non-Hodgkin's lymphoma. Cancer Res 2002;62:3106–12.
5. Kryczek I, Lange A, Mottram P, et al. CXCL12 and vascular endothelial growth factor synergistically induce neoangiogenesis in human ovarian cancer. Cancer Res 2005;65:465–72.
6. Scotton CJ, Wilson JL, Scott K, et al. Multiple actions of the chemokine CXCL12 on epithelial tumor cells in human ovarian cancer. Cancer Res 2002;62:5930–8.
7. Smith MCP, Luker KE, Gargow JR, et al. CXCR4 regulates growth of both primary and metastatic breast cancer. Cancer Res 2004;64:8604–12.
8. Coelho A, Matos A, Catarino R, et al. Protective role of the polymorphism CCR2–64I in the progression from squamous intraepithelial lesions to invasive cervical carcinoma. Gynecol Oncol 2005;96:760–4.
9. Huang J, Wao JL, Zhang L, et al. Differential expression of interleukine-8 and its receptors in the neuroendocrine and non-neuroendocrine compartments of prostate cancer. Am J Pathol 2005;166:1807–15.
10. Makishima H, Ito T, Asano N, et al. Significance of chemokine receptor expression in aggressive NK cell leukemia. Leukemia 2005;19:1169–74.
11. Zafiropoulos A, Crikas N, Passam AM, Spandidos DA. Significant involvement of CCR2-64I and CCL12-3a in the development of sporadic breast cancer. J Med Genet (published online) 23 January 2006.
12. Goldberg-Bittman L, Neumark E, Sagi-Assif O, et al. The expression of the chemokine receptor CXCR3 and its ligand, CXCL10, in human breast adenocarcinoma cell lines. Immunol Lett 2004;92:171–8.
13. Goldberg-Bittman L, Sagi-Assif O, Meshel T, et al. Cellular characteristics of neuroblastoma cells: regulation by the ELR-CXC chemokine CXCL10 and expression of a CXCR3-like receptor. Cytokine 2005;29:105–17.
14. Jones D, Benjamin RJ, Shahsafaei A, Dorfman DM. The chemokine receptor CXCR3 is expressed in a subset of B-cell lymphomas and is a marker of B-cell chronic lymphocytic leukemia. Blood 2000;95:627–32.
15. Kawada K, Sonoshita M, Sakashita H, et al. Pivotal role of CXCR3 in melanoma cell metastasis to lymph nodes. Cancer Res 2004;64:4010–7.
16. Robledo MM, Bartolome RA, Longo N, et al. Expression of functional chemokine receptors CXCR3 and CXCR4 on human melanoma cells. J Biol Chem 2001;48:45098–105.
17. Engl T, Relja B, Blumenberg C, et al. Prostate tumor CXC-chemokine profile correlates with cell adhesion to endothelium and extracellular matrix. Life Sci 2006;78:1784–93.
18. Dexter DL, Kowalski HM, Blazar BA, Fligiel Z, Vogel R, Heppner G. Heterogeneity of tumor cells from a single mouse mammary tumor. Cancer Res 1978;38:3174–81.
19. Trentin L, Agostini C, Facco M, et al. The chemokine receptor CXCR3 is expressed on malignant B cells and mediates chemotaxis. J Clin Investig 1999;104:115–21.
20. Kundu N, Beaty TL, Jackson MJ, Fulton AM. Antimetastatic and antitumor activities of interleukin 10 in a murine model of breast cancer. J Natl Cancer Inst 1996;88:536–41.
21. Kundu N, Fulton AM. Interleukin-10 inhibits tumor metastasis, downregulates MHC class I, and enhances NK lysis. Cell Immunol 1997;180:55–61.
22. Hayakawa Y, Smyth MJ. CD27 dissects mature NK cells into two subsets with distinct responsiveness and migratory capacity. J Immunol 2006;176:1517–24.